TRR
JOURNAL OF THE TRANSPORTATION RESEARCH BOARD

Research Article

Transportation Research Record
1–16

DOI: 10.1177/03611981221086650
journals.sagepub.com/home/trr
SAGE

Evaluation of Geopolymer for Stabilization of Sulfate-Rich Expansive Soils for Supporting Pavement Infrastructure

Jungyeon Jang[1], Nripojyoti Biswas[1], Anand J. Puppala[1], Surya Sarat Chandra Congress[1], Miladin Radovic[2], and Oscar Huang[2]

Abstract

Stabilization of sulfate-rich expansive subgrade soils is a persistent cause of concern for transportation infrastructure engineers and practitioners. The application of traditional calcium-based stabilizers is generally not recommended for treating such soils because of the formation of deleterious reaction products such as ettringite. Sulfate-induced heaving causes severe structural damage to pavements and accounts for enormous expenditure from routine maintenance and rehabilitation activities. A research study was undertaken to evaluate the feasibility of using a metakaolin-based geopolymer (GP) for the treatment of sulfate-rich expansive soil. Laboratory studies were conducted on natural soil and artificially sulfate-rich soils, when treated with either lime or GP, to evaluate and compare the improvements in the engineering properties, including unconfined compressive strength, swelling and shrinkage, and resilient moduli characteristics over different curing periods. Microstructural studies, such as field emission scanning electron microscopy and X-ray diffraction, were performed on treated soils to detect the formation of reaction products. The engineering studies indicate that GP treatment enhanced strength and resilient moduli while suppressing ettringite formation and the associated swell–shrink potential of the treated soils. The microstructural studies showed that GP gels contribute to the improvement of these engineering properties through the formation of a uniform geopolymer matrix. In addition, the absence of a calcium source suppressed the formation of ettringite in the GP-treated soils. Overall, the findings indicate that GPs could be used as a potential alternative to existing traditional stabilizers for treating sulfate-rich expansive soils.

Keywords

Geopolymer, sulfate-rich expansive soil, ettringite, resilient modulus, durability, infrastructure, treated or stabilized soils, pavement, soil stabilization

Expansive soils are prevalent in different parts of the world and cause moderate to severe damage to overlying infrastructures (*1*, *2*). These soils are vulnerable to extensive swelling and shrinkage strains from moisture-induced fluctuations (*3*–*6*). For the past several decades, traditional calcium (Ca)-based stabilizers such as lime has been used to enhance the engineering properties of these soils and mitigate the problems associated with moisture fluctuations (*7*, *8*). Lime treatment helps to improve soil performance through immediate 'modification' reactions, as well as long-term pozzolanic reactions (*9*, *10*). Modification helps to improve the soil plasticity and swell–shrink potentials, changes the soil texture making it friable and workable, and also provides short-term strength. Long-term pozzolanic reactions result in the formation of cementitious compounds such as Calcium-

[1]Zachry Department of Civil and Environmental Engineering, Texas A&M University, College Station, TX
[2]Department of Material Science and Engineering, Texas A&M University, College Station, TX

Corresponding Author:
Anand J. Puppala, anandp@tamu.edu

Silicate-Hydrates (C-S-H) and Calcium-Aluminate-Hydrates (C-A-H), which bind the soil particles into a stabilized matrix and enhance strength, stiffness, and durability (*11*, *12*). Although lime treatment is typically recommended for stabilizing expansive soils, it is inefficient and often counterproductive in the presence of soluble sulfates, such as gypsum and anhydrite, because of the formation of a deleterious mineral, ettringite (*7*, *8*, *13*, *14*). Consequently, traditional Ca-based stabilizers are not recommended for treating expansive soils with soluble sulfate concentrations over 3,000 parts per million (ppm) (*5*, *15*).

Ettringite, $Ca_6(Al(OH)_6)_2(SO_4)_3{\cdot}26H_2O$), a calcium-alumino-sulfate mineral is precipitated when alumina available from the dissolution of clay in alkaline environments ($pH > 10.5$) reacts with Ca^{+2} from Ca-based stabilizers and soluble sulfates in the presence of water (*1*, *12*, *13*, *16*). Stoichiometrically, ettringite crystals could undergo a potential volumetric expansion up to 137% (*7*, *17*). Furthermore, the volumetric expansion could reach up to 250% in Ca-based stabilizer treated sulfate-rich soil layers from the hydration and growth of ettringite when exposed to water (*18*, *19*). The ettringite-induced heaving has detrimental impacts, such as recurrent failures and frequent maintenance of civil infrastructures, including residential buildings and transportation infrastructures (*9*, *14*, *20*). Therefore, research on novel techniques and non-traditional additives is imperative for the effective stabilization of sulfate-rich expansive soils.

Different treatment techniques, including pre-compaction mellowing, double lime application, and utilization of co-additives (e.g., Class F fly ash, ground granulated blast furnace slags, and crystalline silica-rich admixtures), have been investigated for stabilizing sulfate-rich soils (*17*, *20–23*). Even though some of these techniques have shown promising results, most techniques increase the overall construction time because of longer curing periods required for effective performance before moisture exposure (*17*, *24*). Moreover, the use of the majority of such co-additives involves the usage of a substantial amount of Ca-based stabilizers. Therefore, only a limited reduction in greenhouse gas emissions can be achieved (*25*, *26*). Therefore, geotechnical researchers continuously strive to identify different eco-friendly stabilizers that can be used as sustainable alternatives for treating such soils (*19*, *25*, *26*).

Geopolymers (GPs) are attracting attention as promising eco-friendly stabilizers for their ability to improve the strength, stiffness, and swell–shrink characteristics (*19*, *24*, *26–28*). GPs are amorphous inorganic polymers synthesized between 20°C and 90°C (68°F–194°F) by mixing aluminosilicate sources (e.g., clay, metakaolin, fly ash) with an Alkaline Activator Solution (AAS), which consists of alkali metal cation (e.g., KOH, NaOH), water, and silica (optional) (*25*, *26*, *29*, *30*). The aluminosilicate-rich materials, such as metakaolin (MK), fly ash, ground granulated blast furnace slag (GGBFS), and rice husk ash, are used for alkali activation to form inorganic cementitious products (*29*, *31–33*). GPs could be used as eco-friendly treatment alternatives to Ca-based stabilizers since they use industrial by-products as aluminosilicate sources and emit lower carbon dioxide than Ca-based stabilizers. Therefore, the energy consumption from the production and transportation of GP treatment is less than traditional lime treatment (*26*). As a result, the chemical treatment of soil with GPs has been studied extensively by researchers to improve the performance of problematic soils (*25*, *34–37*).

Studies involving low-sulfate clay soils treated with MK-based GP activated with potassium hydroxide (KOH) or with GGBFS-based GP activated with sodium hydroxide (NaOH) mixed with a polypropylene fiber have been shown to improve the strength values after treatment (*25*, *34*). The majority of the literature reports that GP-stabilized soils exhibit significant improvement in engineering properties as compared with conventional stabilizers; however, most of the previous studies were concentrated on soils with no significant concentration of soluble sulfates (*19*, *24*, *25*, *38–40*). Only a few studies evaluated the effects of GP treatment for stabilizing sulfate-rich expansive soils. Moreover, the research objectives of those studies were limited to the effects of GP treatment on swelling or strength properties of the treated soils (*19*, *24*). No major studies have been conducted to evaluate the effects of GP treatment on the resilient modulus and durability aspects of sulfate-rich expansive subgrades. Therefore, research on engineering properties, including strength, durability, swell–shrink potential, and resilient moduli, is necessary to develop a comprehensive knowledge of this novel treatment technique.

An experimental program was undertaken to address the previous research gaps by studying the engineering properties of sulfate-rich expansive soils treated with MK-based GP. The sulfate-rich soils were also treated with lime to provide a comparative analysis between the traditional and the novel treatment methods. An array of laboratory tests, including Unconfined Compressive Strength (UCS) tests with and without moisture conditioning, free swell tests, linear shrinkage tests, and Repeated Load Triaxial Tests (RLTT), were performed on GP-treated, lime-treated and untreated soils to assess the improvement in engineering properties. In addition, Field Emission Scanning Electron Microscopy (FESEM) studies of lime-treated and GP-treated specimens were performed to study the morphological changes after chemical treatments. Further, X-Ray Diffraction (XRD) studies were conducted on untreated and treated soils to

identify the relative changes in the existing mineral peaks and detect the formation of new peaks. The following sections present the materials used for the research study, GP synthesis, engineering, and microstructural tests, and discussion and analysis of the test results.

Materials and Methods

Materials

The natural soils were collected from a cut slope located on the U.S. Highway 75 Frontage road, Grayson County, Denison, TX (33°47′25.5″N 96°34′13.9″W) in February 2020 (Figure 1). The highway embankment experienced minor desiccation cracks since early 2014, and subsequently, a major slope failure occurred in 2016 (*2*). The approach road was shut down immediately after the major failure, and therefore the soil from this location was selected as an ideal geomaterial for this study.

Table 1 and Figure 2 present the basic engineering characterization results and the grain size distribution of the soil, respectively. The natural soil consists of a clay fraction of 57.5%, and liquid limit (LL) and plasticity index (PI) of 60 and 33, respectively. Based on this, the soil is classified as a high plasticity clay (CH) according to the Unified Soil Classification System (USCS). The vertical free swell strain (ASTM D4546) and linear shrinkage strain (Tex-107-E) of the untreated soil were estimated as 12.2% and 15.1%, respectively. The soluble sulfate content of the soil was measured as 336 ppm (Tex-145-E).

The natural soil with a sulfate content of 336 ppm was used to artificially synthesize a high-sulfate soil with a sulfate content of 10,000 ppm by mixing 1.77 g of laboratory-grade gypsum ($CaSO_4{\cdot}2H_2O$) per 100 g of natural dry soil. The sulfate concentration of 10,000 ppm was deemed suitable to classify the soil as a high-sulfate soil (sulfate content > 8,000 ppm) based on TxDOT guidelines (*41*). Therefore, in this study, the natural low-sulfate soil is abbreviated as LS, and the artificially synthesized high-sulfate soil is abbreviated as HS.

GP Synthesis and Optimum GP Composition

GP synthesis requires an aluminosilicate source and AAS. In this study, MK was used as the aluminosilicate precursor because it is relatively pure compared with other aluminosilicate precursors. The AAS was prepared by mixing KOH, deionized water, and amorphous fumed silicon (IV) oxide (silica fume). During AAS synthesis, KOH flakes were first dissolved in deionized water to separate K^+ and OH^- and subsequently increase the pH of the solution. Subsequently, a certain percentage of silica fumes were added to the solution to ensure a desired ratio between Si and Al (53.0% silicon and 43.8% aluminum) before mixing with the MK precursor. Further, the AAS, containing KOH and silica fumes, was mixed by a magnetic stirrer for at least 48 h at room temperature until it became a viscous solution. The AAS was stored in sealed containers immediately after mixing to minimize contamination from atmospheric carbonation. Subsequently, MK and the AAS were uniformly mixed for at least 3 mins to prepare a homogeneous solution with the target ratio of Si to Al. Based on some preliminary trials, a GP composition consisting of $SiO_2/Al_2O_3 = 3$, water/solid = 3, and K/Al = 1 was deemed suitable for treating this soil. The optimum GP composition was abbreviated as K331 (where K indicates alkali

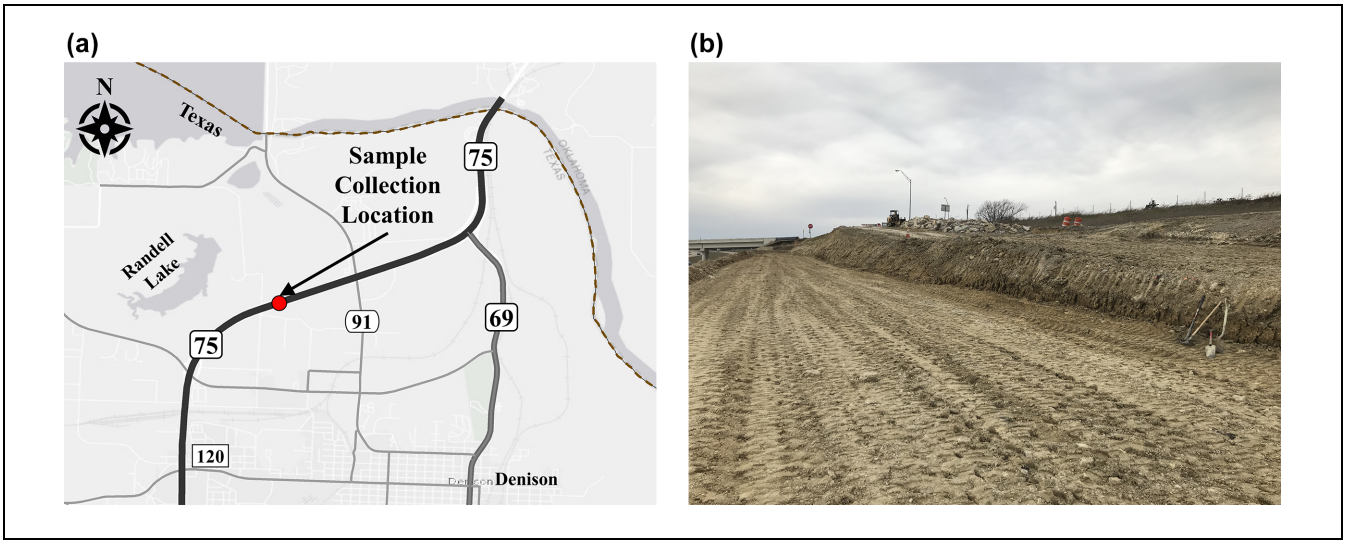

Figure 1. Location of soil sample collection in Denison, Texas: (*a*) map of location, (*b*) photograph of site in February 2020.

Table 1. Basic Geotechnical Properties of Natural Soil Used in This Study

Property	Standard	Unit	Value
Specific gravity, G_S	ASTM D854	NA	2.72
Clay content	ASTM D7928	%	57.5
Silt content	ASTM D7928	%	34.2
Unified Soil Classification System (USCS)	ASTM D2487	NA	CH (fat clay)
Liquid Limit (LL), Plasticity Index (PI)	ASTM D4318	%	60, 33
Optimum Moisture Content (OMC)	ASTM D698	%	20.0
Maximum Dry Density (MDD)	ASTM D698	g/cm^3	1.66
Vertical free swell strain	ASTM D4546	%	12.2
Linear shrinkage strain	Tex-107-E	%	15.1
Soluble sulfate content	Tex-145-E	ppm	336

Note: 1 g/cm^3 = 62.4 pounds per cubic foot; ASTM = American Society for Testing and Materials; NA = Not Available; Tex = Texas Department of Transportation; ppm = parts per million.

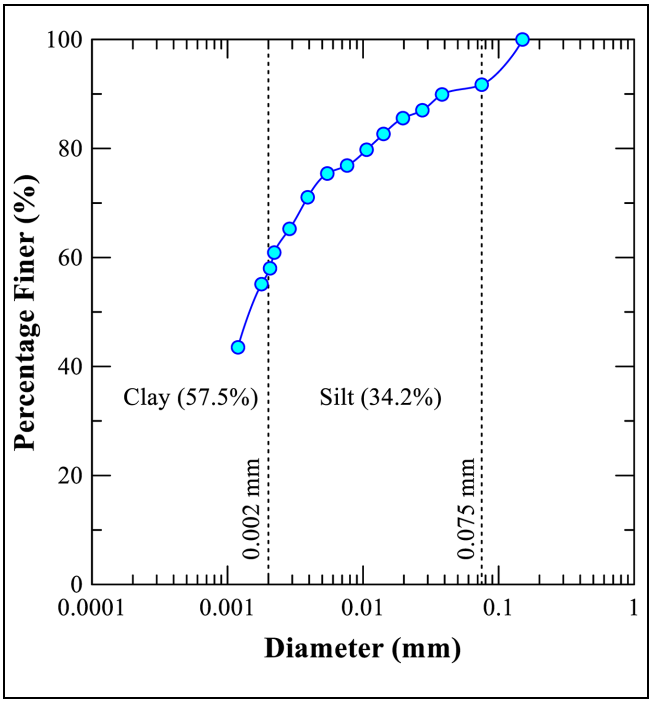

Figure 2. Grain size distribution of natural soil.

source, i.e., KOH, and the digits indicate the ratios of different components discussed earlier) in this study.

Specimen Preparation

The collected soils were air-dried, crushed, and pulverized for this study. The optimum lime dosage was selected as 6% lime by dry weight of the soil, based on the Eades and Grim method (ASTM D6276). Lime-treated specimens were prepared by evenly mixing the appropriate lime dosage, dry soil, and target moisture content. For GP-treated soils, the GP dosages used in this study were expressed as a percentage of the total mass of the GP (includes MK, KOH, silica fume, water) to the dry weight of the soil to be treated with GP. Thus, 8% and 30% GP dosages were selected to evaluate the efficacy of GP treatment on soil properties. The target dosage of the GP slurry was mixed with dry soil, and then the mixture was placed in a sealed plastic bag to prevent moisture evaporation during the specimen preparation. Depending on the type of engineering tests, different molding times were recorded for specimen preparation (e.g., UCS and durability tests: $\approx$ 10 mins; free swell tests and RLTT: $\approx$ 30 mins). In addition to the treated specimens, untreated soil specimens were also prepared for comparative studies. The lime-treated specimens were abbreviated as 6L-(LS/HS) specimens, and the GP-treated specimens were abbreviated as (8/30)GP-(LS/HS) for the subsequent study.

The moisture content–dry density relationships were determined for each treatment using static compaction in the Harvard miniature compaction apparatus (Figure 3). Untreated, lime-treated, and GP-treated specimens were prepared by statically compacting the specimens at 98% MDD and wet side of OMC (Table 2). The chemical reactions involved to complete the process of geopolymerization require a significant quantity of water. Therefore, the specimens were prepared on the wet side of OMC to ensure that the reactions were not hindered (*42*). In addition, specimens were prepared as required by RLTT, UCS tests, free swell tests, shrinkage tests, volume change measurements (before and after capillary soaking), and microstructural characterization studies (FESEM, XRD) to evaluate the effects of GP treatment on strength, stiffness, and durability. All laboratory tests were performed on the specimens cured for three different curing periods of 0 day (6 h), 3 days, and 14 days to understand the effect of the curing period on chemical treatments. The specimens were cured at room temperature (23.5 $\pm$ 0.5°C or 74.3 $\pm$ 0.9°F) in hermetically

Table 2. Target Dry Density and Moisture Content for Each Specimen Group

Soil group	Type of stabilizer	Dosage (%)	Specimen group	OMC (%)	MDD (g/cm^3)	MC at 98% MDD (%)	98% MDD (g/cm^3)
Low-sulfate (LS)	Lime (L)	6	6L-LS	30.0	1.47	33.2	1.44
	Geopolymer	8	8GP-LS	28.1	1.45	31.0	1.41
	(GP)	30	30GP-LS	24.6	1.56	25.1	1.53
High-sulfate (HS)	Lime (L)	6	6L-HS	30.0	1.47	33.2	1.44
	Geopolymer	8	8GP-HS	28.1	1.45	31.0	1.41
	(GP)	30	30GP-HS	24.6	1.56	25.1	1.53

Note: 1 g/cm^3 = 62.4 pounds per cubic foot; OMC = optimum moisture content; MC = moisture content; MDD = maximum dry density.

sealed plastic bags ($\approx$ 100% relative humidity) to prevent moisture loss during the chemical reactions. As the curing temperature strongly affects the process of geopolymerization, curing the specimens at the standard temperature was deemed necessary to replicate the in-situ curing conditions (*43*, *44*).

Experimental Studies

Strength and Durability Studies

The UCS tests were conducted to assess the strength improvements of the treated soil. A total of six soil specimens were prepared for each curing period and tested. The UCS tests were conducted on three of the six specimens immediately after each curing period. The remaining three specimens were tested for UCS after they had been subjected to capillary soaking for 48 h. The UCS tests on the untreated and treated soil specimens (diameter: 33 mm or 1.3 in., and height: 67 mm or 2.6 in.) were performed on the specimens at a strain rate of 1%/min, as per ASTM D2166.

The changes in the UCS of specimen groups with the curing period demonstrated the strengthening effect of GP over the traditional stabilizer. In addition, the soaked UCS properties provided a better understanding of the effects of moisture intrusion and potential ettringite-induced damage. The changes in UCS of treated specimens before and after capillary soaking were calculated as the strength retention factor (S_R) (Equation 1) (*45*).

$$S_R = \frac{UCS_{(unsoaked)}}{UCS_{(soaked)}} \times 100\ (\%) \qquad (1)$$

where $UCS_{(unsoaked)}$ = UCS values of the specimens before capillary soaking; and $UCS_{(soaked)}$ = UCS values of the specimens after capillary soaking. The S_R factor after moisture exposure provided an indirect comparison between the durability of GP-treated soils over lime-treated soils.

Swelling and Shrinkage Properties

The swelling characteristics of lime and GP-treated soils were investigated with volumetric swell measurements after capillary soaking and the free swell strains from free swell tests. Compared with lime treatment, the changes in the swell strains indicate the influence of GP treatment on both LS and HS groups. The volumetric swell (V_S) factor was measured using the differences between the diameter and height before and after capillary soaking. UCS specimens before and after capillary soaking were used to measure the volume changes for each curing period.

Free swell tests were performed on different soil groups of untreated and treated soil specimens. For each specimen group and curing period combination, duplicate specimens of 63.5 mm (2.5 in.) diameter and 25.4 mm (1.0 in.) height were prepared by static compaction. Free swell tests were performed under vertical stress of 1 kPa as per ASTM D4546 and recorded by the dial gauge. The dial gauge readings were recorded until no change in the readings was observed for three consecutive days.

The linear shrinkage tests were conducted as per Tex-107-E to investigate the shrinkage behavior of untreated and treated soils. Dried untreated soils passing sieve #40 (sieve size: 0.475 mm) and treated soils after each curing period were mixed with distilled water until a consistency close to the liquid limit was obtained. To prevent soil from sticking to the walls of the mold, petroleum jelly was used to grease the walls. Finally, the mold was filled with the slurry and placed at room temperature. After the change in color of the specimen, the mold was dried in an oven for 24 h at 110 $\pm$ 5°C (230 $\pm$ 9 °F). The lengths of the dried specimens were measured precisely to determine the linear shrinkage strain of the soil specimens.

Stiffness Properties

Resilient modulus (M_R) is the stiffness property of pavement materials and is an important input parameter for characterizing flexible and rigid pavement design by the

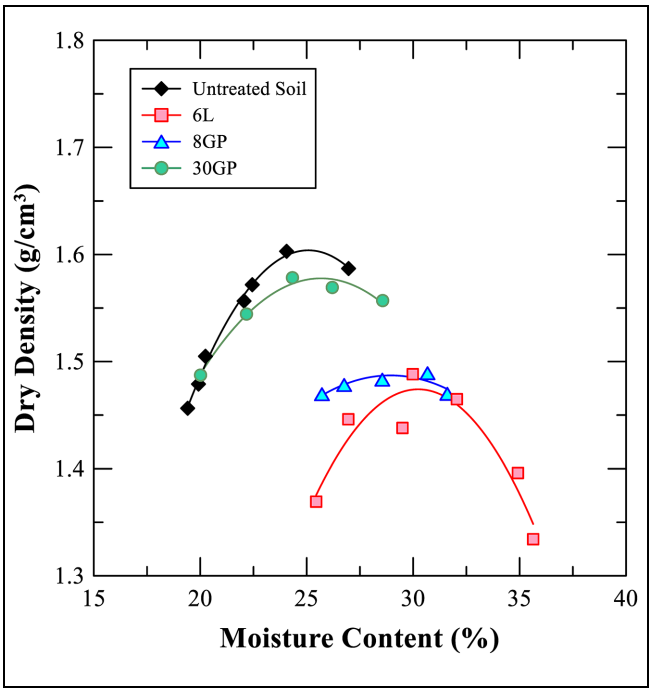

Figure 3. Moisture content–dry density relationship for untreated soil, lime- and geopolymer-treated soils.

Mechanistic-empirical (M-E) Pavement Design Guide manual. In addition, the M_R values are used to estimate the thickness of pavement layers and the overall response of the pavement to traffic loadings for long-term pavement performance. Since the primary focus of this study was the treatment of high-sulfate soils, RLTT was conducted on cylindrical specimens (diameter: 72 mm or 2.83 in., and height: 148 mm or 5.83 in.) of untreated, 6L-HS, 8GP-HS, and 30GP-HS groups as per AASHTO T-307. Duplicate specimens for each soil group and three curing periods were prepared to evaluate the respective resilient moduli properties and provide a comprehensive understanding of the novel stabilizer on sulfate-rich soils.

Microstructural Characterization

Microstructural studies using FESEM and XRD were performed on treated high-sulfate soils and compared with untreated soils to investigate the stabilization mechanisms and ettringite formation. FESEM studies were utilized to observe morphological changes of the treated specimens (diameter: 33.3 mm or 1.3 in., and height: 22.4 mm or 0.9 in.) cured for 14 days. Since the FESEM studies provide only visual indications in relation to the changes in soil morphology, additional studies using XRD were performed on untreated and treated soil groups to detect the mineralogical changes before and after chemical treatment. XRD studies were conducted using Cu-Kα radiation source at 10 mA and 30 kV, with a range of 2θ from 10° to 60° and a step size of 0.02°.

Analysis and Discussions

This section discusses the results from engineering, mineralogical, and microstructural studies. Results from engineering and microstructural characterization studies help in the development of a comprehensive understanding of this novel treatment method.

Strength and Durability Studies

The unsoaked and soaked UCS values of the treated LS and HS specimen groups for different curing periods are represented in Figures 4 and 5. The unsoaked and soaked UCS values of the untreated soil were measured at 144.9 kPa (21.0 pounds per square inch [psi]) and 13.0 kPa (1.9 psi), respectively. Lime and GP treatments significantly improved the UCS as compared with untreated soil. Modification and pozzolanic reactions in 6% lime-treated soil results in strength enhancement from the formation of cementitious reaction products, which bind the soil solids into a strong matrix. Similarly, for 30% GP, the formation of a strong GP network from geopolymerization and uniform coating of soil particles resulted in strength enhancement after all curing periods. The strength-enhancing effect of 30% GP treatment is significantly greater than that of 6% lime treatment. However, the UCS values of 8% GP treatment are similar to or lower than those of 6% lime-treated soils. Because of the low dry density and high moisture content compared with 30% GP, the moisture in the pores created between the clay particles possibly interfered with the geopolymerization process and resulted in the partial formation of the GP network. When subjected to capillary soaking, all treated specimens showed a reduction in strength from the weakening of the bonds. The effects of moisture intrusion are explained in relation to retained strength in the following paragraph.

The engineering properties of the treated specimens degenerated after moisture intrusion. Figure 6 represents S_R factors of LS and HS specimens treated with lime or GP for various curing periods. In low-sulfate soils, the cementitious gels formed over the curing period were responsible for preventing moisture intrusion during capillary soaking and preventing strength loss (Figure 6*a*). However, in HS soils, the nucleation and growth of ettringite crystals on moisture conditioning were responsible for damaging the cementitious bonds formed in the soil, and therefore there is a significant loss of strength even after a longer curing period (Figure 6*b*).

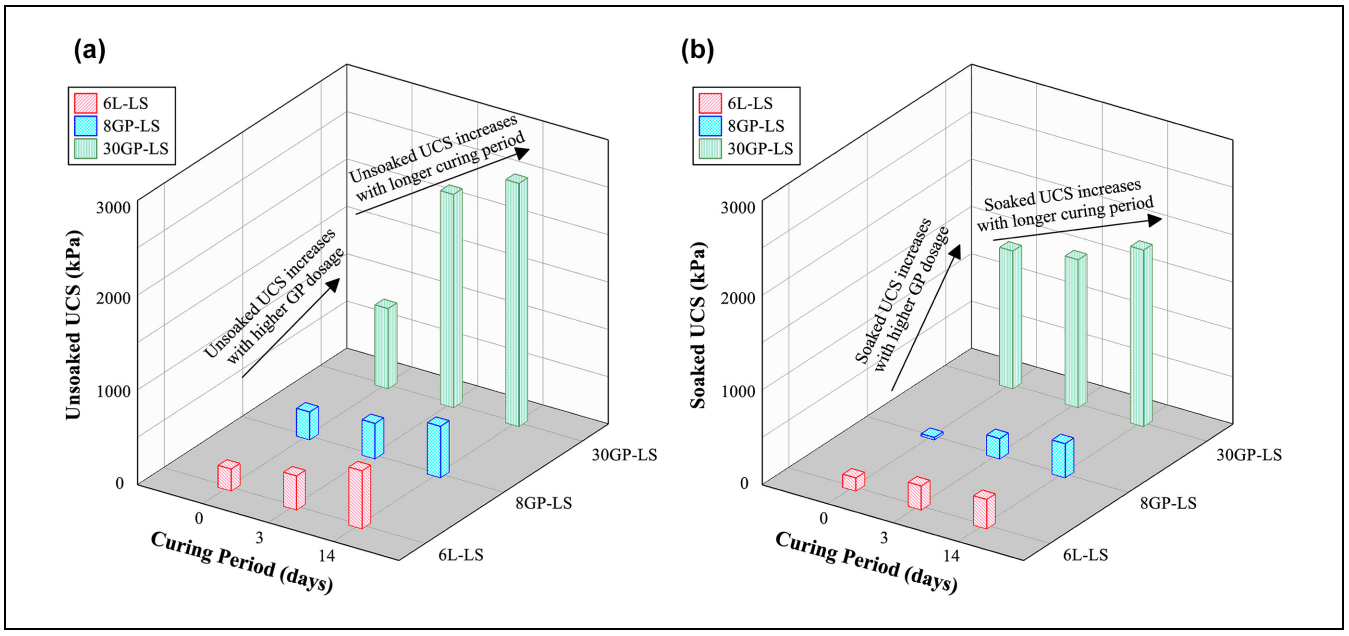

Figure 4. Unconfined Compressive Strength (UCS) test results of the low-sulfate soil (LS) specimen group: (*a*) unsoaked UCS and (*b*) soaked UCS.

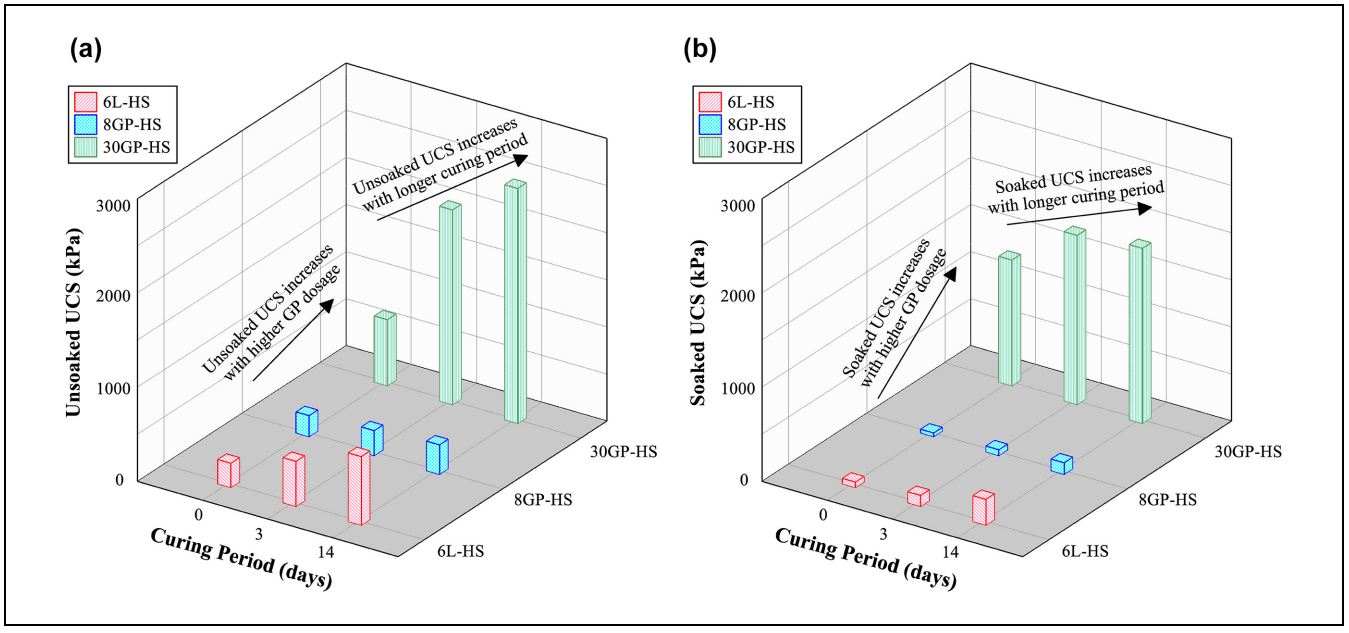

Figure 5. Unconfined Compressive Strength (UCS) test results of the high-sulfate soil (HS) specimen group: (*a*) unsoaked UCS and (*b*) soaked UCS.

A 30% GP treatment provided significant strength retention factors for both LS and HS soils in GP treatment. The uniform coating of soil particles and the formation of strong bonds from geopolymerization prevented moisture intrusion into the soil and helped to retain 172%–190% strength for 0 day curing and 69%–87% strength for 3 and 14 days curing (Figures 6*a* and 6*b*). Furthermore, the absence of ettringite (since no Ca-based source), which is a hydrophilic mineral, also provided additional benefits during moisture conditioning. The results also indicate that the soaked UCS of 30GP-LS and 30GP-HS specimens cured for 0 day was higher than the unsoaked UCS. This unusual behavior could possibly be attributed to accelerated geopolymerization

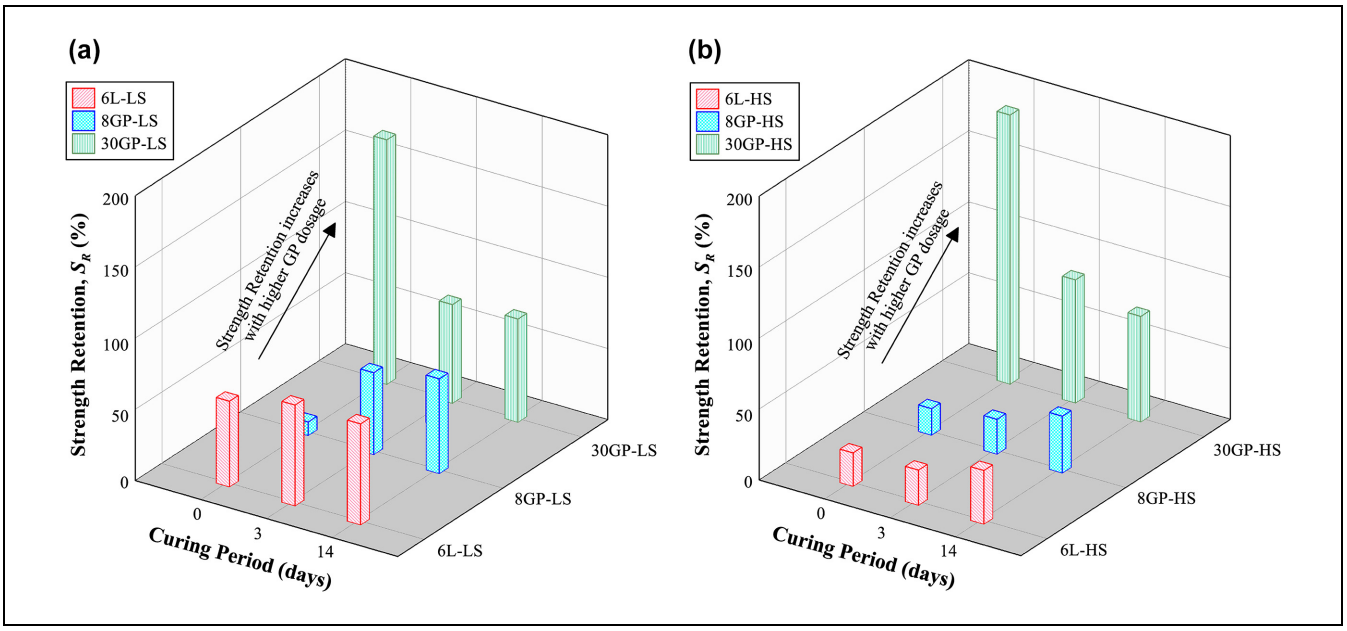

Figure 6. Strength Retention (S_R) factors: (*a*) low-sulfate (LS)-treated and (*b*) high-sulfate (HS)-treated specimens with lime and geopolymer (GP).

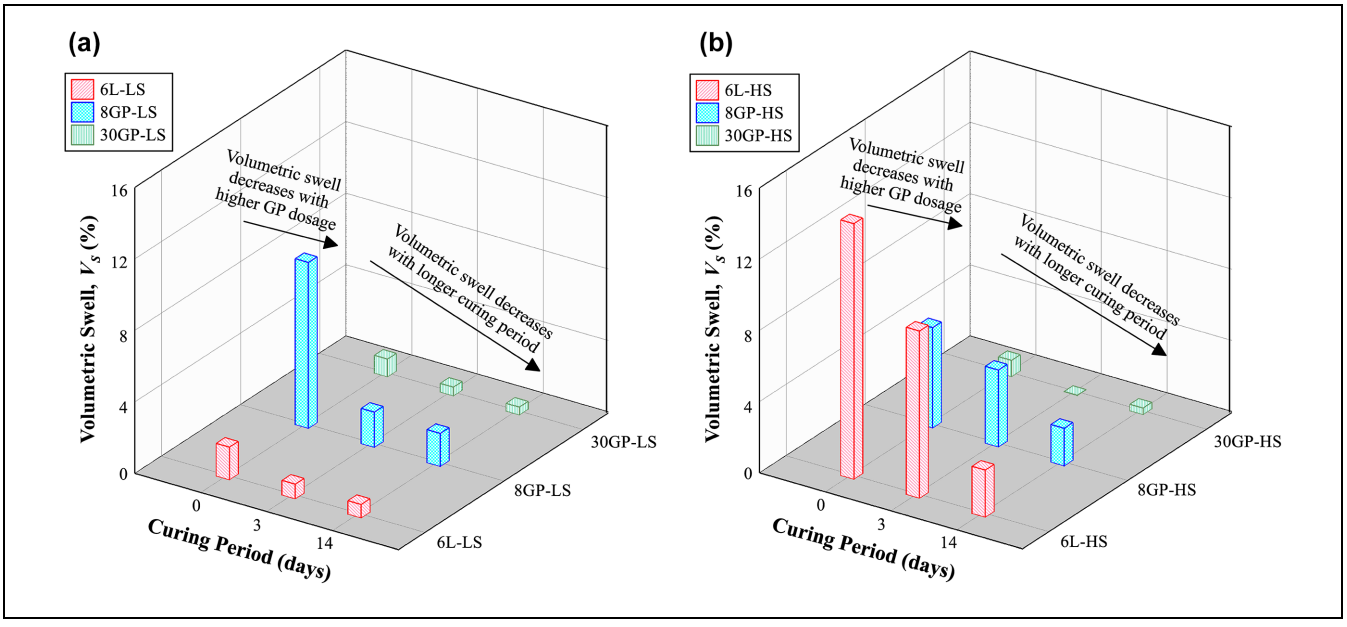

Figure 7. Volumetric Swell (V_S) factors: (*a*) low-sulfate (LS)-treated and (*b*) high-sulfate (HS)-treated specimens with lime and geopolymer (GP).

after supplying additional moisture to GP gels. However, no conclusive evidence was obtained to explain this behavior for such a high dosage of GP. In the specimens treated with 8% GP, it was observed that the S_R value was much lower than both traditional treatments as well as 30% GP treatment (Figures 6*a* and 6*b*). Insufficient GP dosage and inability to uniformly coat the soil particles resulted in deterioration of the bonds when subjected to capillary moisture. Therefore, it could be observed that the higher dosage of GP treatment provided a better performance on the durability aspects as compared with 6% lime treatment for both sulfate levels.

Swelling and Shrinkage Properties

The V_S values of LS and HS soils treated with lime and GP are shown in Figure 7. For soil with a low concentration of soluble sulfate, both lime and higher dosage of

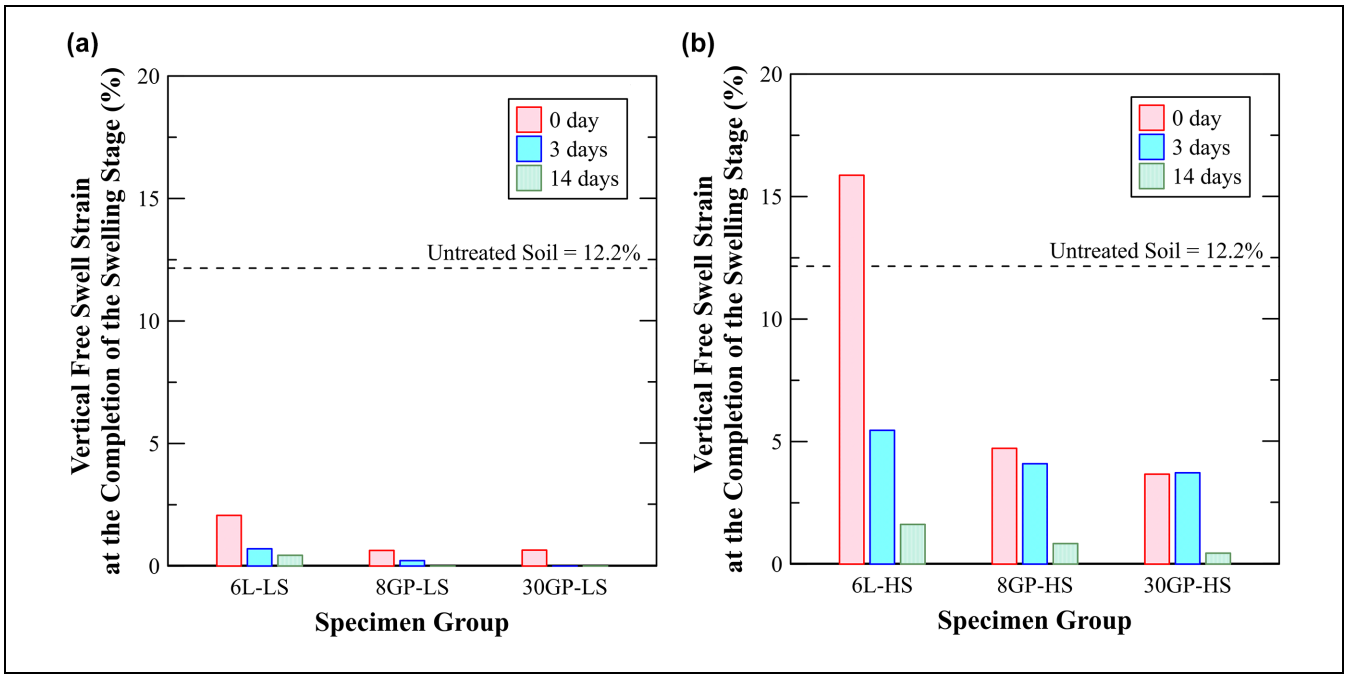

Figure 8. Vertical free swell strain test results: (*a*) low-sulfate soil (LS) specimen group and (*b*) high-sulfate soil (HS) specimen group.

GP treatment were effective in reducing the V_S values from the early curing period. However, 8% GP-treated soils showed greater swelling than other treatment methods as a result of insufficient coating, which possibly resulted in poor strength performance, as seen in Figure 4*b*. The nucleation and growth of ettringite crystals inside the 6L-HS soil resulted in an increase in the V_S values of the treated soil even after a longer curing period (Figure 7*b*). Treating the sulfate-rich soil with 30% GP resulted in a significant decrease in the V_S values immediately after treatment. The uniform coating of soil particles and the formation of strong bonds from geopolymerization prevented the swelling of specimens even during the early curing periods. The overall reduction in the V_S values in addition to higher retained strength (Figure 6*b*) imparts significant durability to GP-treated HS soils.

The vertical free swell strains of both LS and HS soils subjected to different treatments are shown in Figure 8. Lime or GP treatment significantly reduced the swelling potential for LS soils (Figure 8*a*). No vertical free swell was recorded in 8% GP and 30% GP specimens after 14 days and 3 days of curing, respectively. The formation of cementitious compounds for 6% lime treatment, geopolymerization reactions, and the formation of GP networks could be attributed as primary factors for such improvements. However, the ettringite-induced heaving for sulfate-rich soils causes significant swelling even after a longer curing period (Figure 8*b*). A 30% GP treatment positively affected the reduction of swelling potential even during the curing period. The absence of a Ca-based source to form ettringite and the uniform coating of clay particles from GP gels during geopolymerization and the development of stronger bonds possibly prevented the swelling in these soils.

Figure 9 shows the linear shrinkage test results for different treatments on the overall curing of LS and HS soils. In lime-treated and GP-treated soils, an immediate reduction in linear shrinkage strain was observed for both low and high soluble sulfate soils. Lime treatment reduces the linear shrinkage strains of the LS and HS groups immediately because of a reduction in moisture affinity from cation exchange on the clay surface. However, no major changes in shrinkage percentage were noted over a longer curing period. An 8% GP treatment showed superior (Figure 9*a*), or comparable (Figure 9*b*) performance to 6% lime-treated soils, potentially from partial GP coating of the cohesive soils and subsequent development of cohesionless behavior. In contrast, 30% GP treatment significantly reduced the shrinkage strains as the fully-formed network of GP gels was able to uniformly coat the clay particles and reduce their water affinity. A 30% GP treatment in LS and HS specimens cured for 14 days changed the behavior of the soil from cohesive to cohesionless; therefore, these soils could not be tested following the standard testing protocols. Compared with 6% lime and 8% GP treatments, 30% GP treatment reduced significant shrinkage potential over longer curing periods. Therefore, from the above discussion, it could be observed that higher GP dosage and a longer curing period have a significant potential to reduce the linear shrinkage strains.

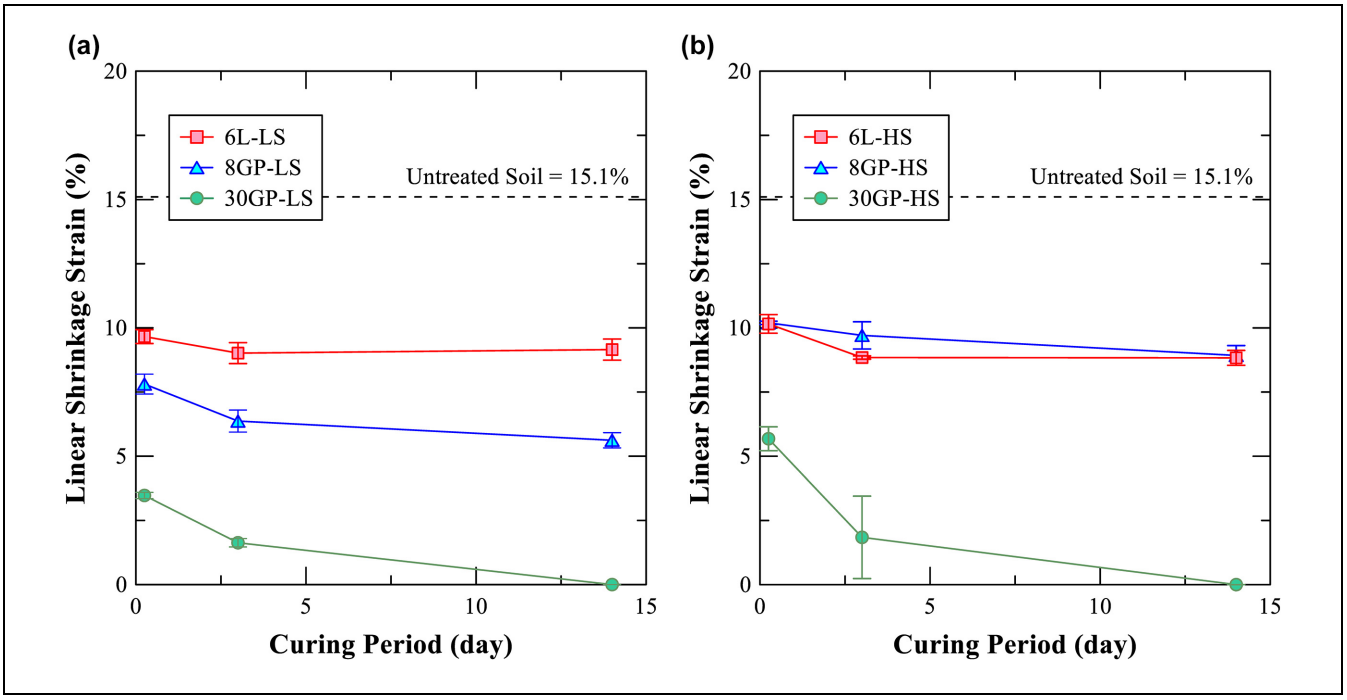

Figure 9. Linear shrinkage strain test results: (*a*) low-sulfate soil (LS) specimen group and (*b*) high-sulfate soil (HS) specimen group.

Table 3. Resilient Modulus Properties: Universal Model Constants and Coefficient of Determination

Curing period	0 day				3 days			14 days		
Model constant	Untreated soil	6L-HS	8GP-HS	30GP-HS	6L-HS	8GP-HS	30GP-HS	6L-HS	8GP-HS	30GP-HS
k_1	627	684	1054	1796	1502	1469	2659	1739	1469	3123
k_2	0.617	0.411	0.214	0.124	0.221	0.263	0.266	0.356	0.206	0.329
k_3	−5.189	−3.591	−1.448	0.038	−0.210	−0.939	0.286	−0.126	−0.143	0.354
R^2	0.976	0.986	0.964	0.933	0.900	0.989	0.961	0.962	0.932	0.903

Note: k_1, k_2, and k_3 are model constants. L = lime; HS = high-sulfate soil; GP = geopolymer.

Stiffness Properties

From the previous studies, it could be observed that both lime and GP treatments have a comparable influence on LS soils. However, GP has a significant influence in improving the strength, durability, and swell-shrinkage properties of HS soils compared with lime treatment. Consequently, RLTT was performed on high-sulfate soils with different GP dosages and compared with lime treatment to understand the effects on resilient modulus properties. Table 3 represents the resilient modulus properties of different treated soil groups in relation to the universal model constants (k_1, k_2, and k_3) with the coefficient of determination (R^2). Having high accuracy, predictive stability, and easy implementation, the model is strongly recommended for pavement design and analysis as per NCHRP project 1-37A (*46*, *47*). The universal model is represented as follows (Equation 2) (*46*, *47*).

$$M_R = k_1 P_a \left(\frac{\theta}{P_a}\right)^{k_2} \left[\left(\frac{\tau_{oct}}{P_a}\right) + 1\right]^{k_3} \quad (2)$$

where M_R = resilient modulus; k_1, k_2, and k_3 = model constants; θ = bulk stress; P_a = atmospheric pressure; τ_{oct} = octahedral shear stress = $\frac{1}{3}\sqrt{(\sigma_1-\sigma_2)^2+(\sigma_2-\sigma_3)^2+(\sigma_3-\sigma_2)^2}$; and $\sigma_2 = \sigma_3$ for axisymmetric stress conditions.

The k_1 values are directly related to the elastic modulus of the specimens. The k_1 values increased with increasing curing period for both lime and GP treatments. The changes in k_1 values of the lime-treated soils could be attributed to the flocculation of clay particles from modification reactions and long-term pozzolanic reactions and the formation of cementitious gels. Additionally, the nucleation of ettringite crystals could have also partially contributed to the improvement in

stiffness values. The k_1 values of GP-treated specimens increased with an increase in the curing period. However, the k_1 values of 30GP-HS at 0-day curing are significantly higher than 6% lime and 8% GP treatments, and also, the rate of change of the k_1 values with curing period is much higher than the other treatments. The possible reasons for these results in GP treatment could be attributed to the short-term agglomeration of clay particles by GP gels and the bonding of the GP gel-clay systems, which becomes stronger with geopolymerization over time. However, the k_1 values of 8GP-HS become almost a plateau after three days of curing. Such behavior could be explained by the formation of a partial coating of GP gels and less geopolymerization as compared with 30% GP treatment.

The effect of bulk stress on treated soil is explained by the k_2 values of lime and GP treatments. However, from the present analyses of k_2 values, no distinguishable trend could be noted for either lime-treated or GP-treated specimens. The k_3 values are affected by shear stress acting in the specimens and are commonly negative. The higher k_3 values for all curing periods for the 30GP-HS specimen indicate possibly higher shear resistance than other treated groups. This could be attributed to the development of uniform coatings of GP matrix because of higher dosage of treatment and the geopolymerization effect during curing. Overall, 30% GP dosage has a significant influence on resilient modulus properties compared with only traditional stabilizers.

M_R variations with confining pressure and deviatoric stress for untreated soil and treated HS specimens cured for 14 days (6L-HS-14d and 8/30GP-HS-14d) are represented in Figure 10. M_R values for the untreated soil decreased with an increase in deviatoric stresses because of the softening behavior of clay soils (Figure 10*a*). This could be explained because loose clay particles were easily affected by the deviatoric stress, and consequently, M_R values decreased as the deviatoric stress increased. Figures 10*c* and 10*d* show the M_R values of the 6% lime-treated HS specimens cured for 14 days. Unlike the untreated soil, the M_R values of the 6% lime-treated soil increased with an increase in deviatoric stresses (Figure 10*c*). This behavior is common in 6% lime-treated soils and could be attributed to the cementation effect between the reaction products and clay particles, which provides a significant contribution in increasing the stiffness of the lime–clay system. Figures 10*e* and 10*f*, display M_R values of 8GP-HS-14d, which change according to the deviatoric stress and confining pressure. As GP gels can provide additional bonding networks surrounding the clay particles, it significantly reduces recoverable strain values (ε_r). Therefore, the M_R values of the 8GP-HS-14d were markedly higher than those of untreated soil. However, a partially-formed GP network fails to exhibit the same hardening behavior as 6% lime-treated soil. Unlike 8% GP treatment, 30% GP treatment showed greater M_R values at higher confining pressure and deviatoric stress than 6% lime treatment (Figures 10*g* and 10*h*). Fully-developed and uniformly-coated GP gels around the clay particles probably strengthen the bonds and could have contributed to an increase in stiffness. In summary, 30% GP treatment significantly improved M_R values and showed a more pronounced hardening effect than traditional Ca-based treatment.

Microstructural Characterization

Microstructural characterization studies using FESEM were performed on HS soil to understand the morphological changes caused by the formation of new reaction products. Figure 11 shows FESEM images of untreated, 6L-HS-14d, and 30GP-HS-14d specimens. The untreated soil is shown in Figure 11*a*; it primarily indicates open pore structures with flaky particles typical of clayey soil. The 6L-HS-14d specimen subjected to moisture conditioning is shown in Figure 11*b*. The characteristic needle-shaped ettringite crystals could be observed in the specimen. The nucleation and growth of these ettringite crystals after moisture intrusion could be considered a primary factor for the relatively poor performance of 6% lime-treated specimens. The 30GP-HS specimens in Figure 11*c* show remarkably different morphology after 14 days of curing. The clay particles are observed to be coated with uniform layers of GP matrix. These uniform coatings might have been responsible for providing physical bonding to hold the loose clay particles and impart significant improvement in engineering properties. Also, the absence of ettringite crystals in GP-treated soils might have resulted in minimal deterioration of engineering properties after moisture conditioning. It should be noted that the differences in color and brightness in the images generated from secondary electron beams are primarily caused by the rough texture of the surface instead of any chemical or mineralogical differences (*48*). To further verify the mineralogical changes, additional studies using XRD were performed as discussed below.

The X-ray diffractograms of untreated, lime-treated, and GP-treated specimens after curing the specimens for 14 days and subjecting them to moisture conditioning are shown in Figure 12. The untreated natural soil is primarily showing diffraction peaks of calcites (29.4°, 36.1°, 43.2°, 47.6°, 48.6°, 57.5°), quartz (20.9°, 26.6°, 39.5°, 42.5°, 50.2°), illite (19.9°, 24.9°, 35.0°), muscovites (17.9°), and some montmorillonite (19.9°, 23.1°). No characteristic peaks of mineral gypsum were observed in the natural soil (sulfate content = 336 ppm). The artificially synthesized HS soil treated with 6% lime is shown in Figure 12*b*. The addition of gypsum and lime resulted

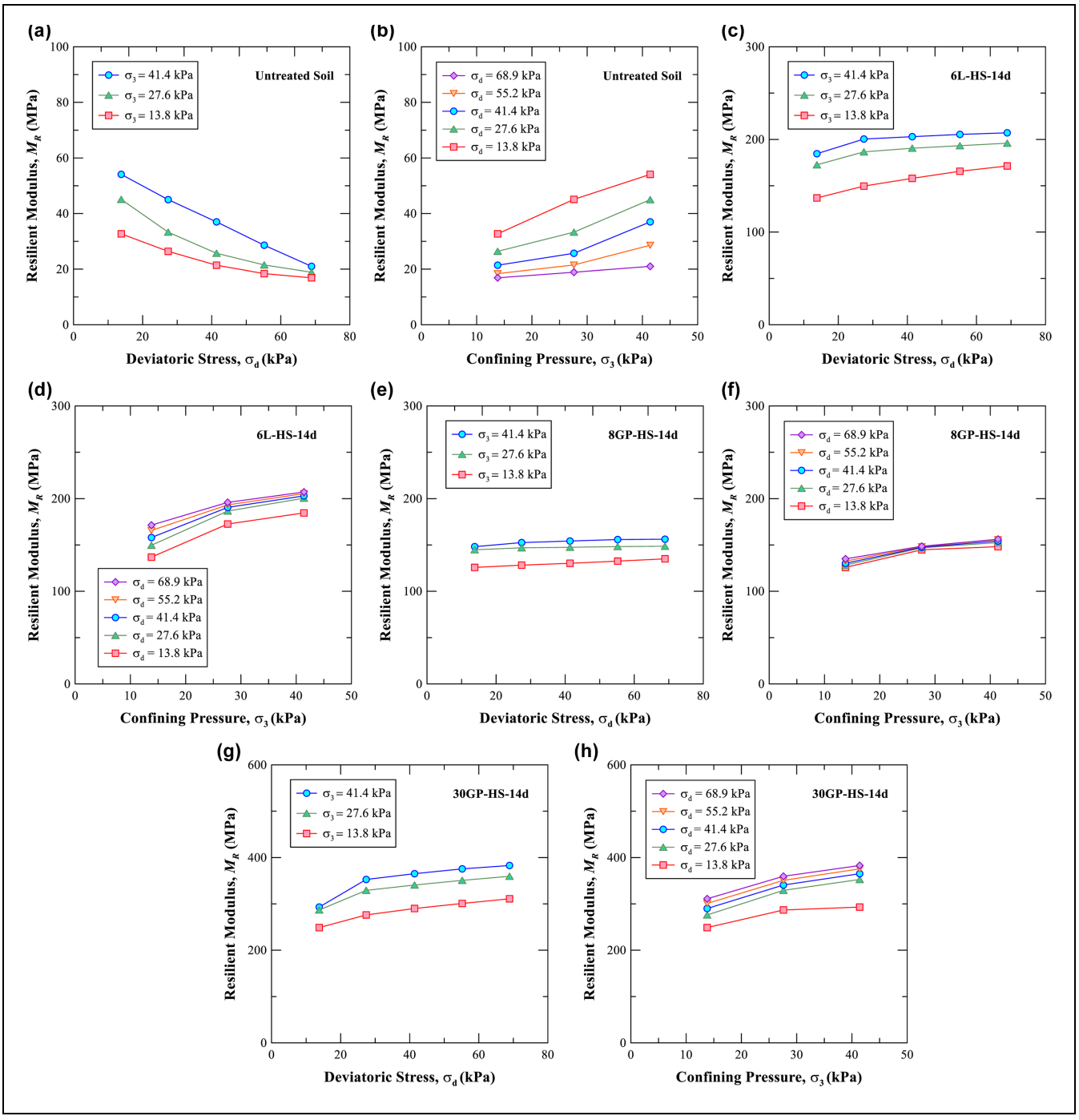

Figure 10. Resilient modulus (M_R) variations with deviatoric stress and confining pressure for: (*a*, *b*) untreated soil, (*c*, *d*) 6L-HS-14d, (*e*, *f*) 8GP-HS-14d, and (*g*, *h*) 30GP-HS-14d.

Note: L = lime; HS = high-sulfate soil; GP = geopolymer.

in the development of new peaks, as observed in the diffractogram. The characteristic gypsum peak (11.7°) could still be observed after 14 days of curing. In addition to the gypsum peak, peaks at 15.8° and 18.6° confirmed ettringite formation in HS soil as observed in the FESEM image (Figure 11*b*). The soluble sulfate from gypsum, Ca^{+2} from lime, and soil aluminates under high pH react in the presence of moisture to form this deleterious mineral which imparts significant strength loss and volumetric swell in 6% lime-treated HS soils even after longer curing periods (Figures 6*b* and 7*b*). It should be noted that, even though cementitious compounds (e.g.,

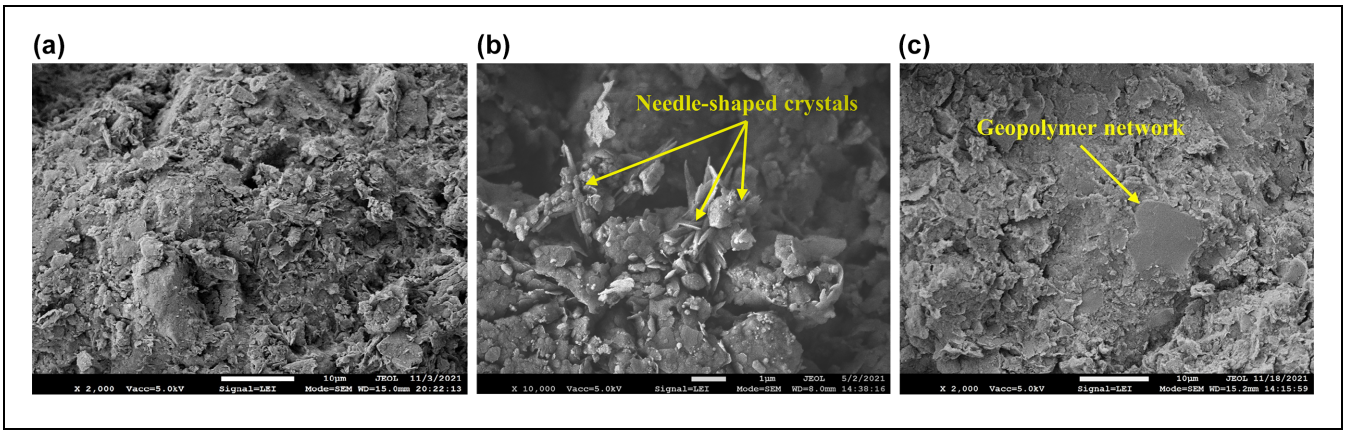

Figure 11. Field Emission Scanning Electron Microscopy (FESEM) images: (*a*) untreated soil, (*b*) 6L-HS-14d, and (*c*) 30GP-HS-14d.
Note: L = lime; HS = high-sulfate soil; GP = geopolymer.

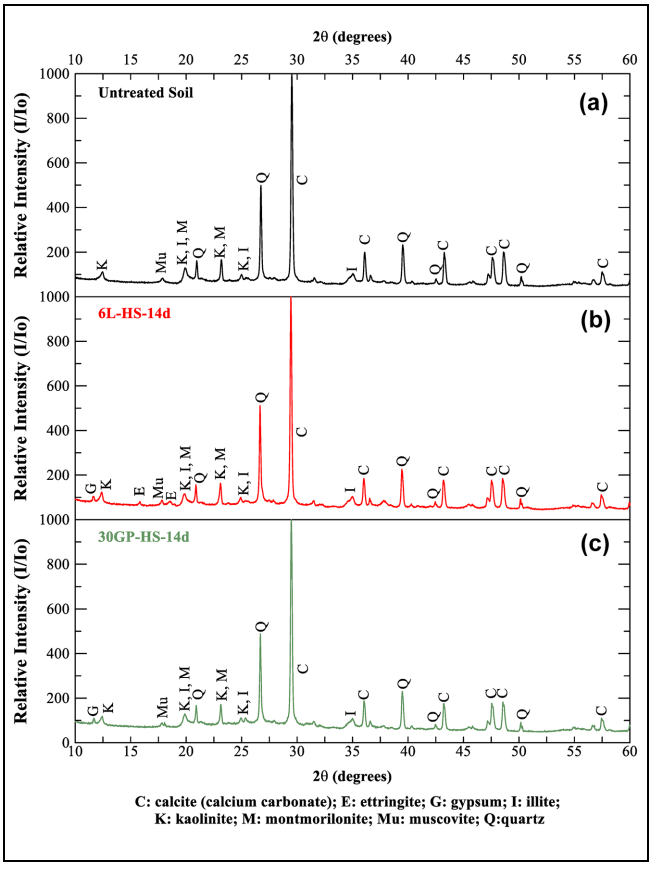

Figure 12. X-Ray Diffraction (XRD) patterns: (*a*) untreated soil, (*b*) 6L-HS-14d, and (*c*) 30GP-HS-14d.
Note: L = lime; HS = high-sulfate soil; GP = geopolymer.

C-S-H) might have formed in the specimen, because of its amorphous nature, no distinguishable peaks were identified. The GP-treated soil (Figure 12*c*) shows the presence of a new gypsum peak at 11.7° from artificially treating the natural soil with $CaSO_4{\cdot}2H_2O$. However, in the absence of a Ca-based source, no ettringite peaks were formed in 30GP-HS-14d, indicating the efficacy of this novel stabilizer in suppressing the formation of ettringite, imparting significant improvements in other engineering properties (Figures 5, 8, 9, and 10).

Summary and Conclusion

This study conducted tests to understand the efficacy of using a novel metakaolin-based GP to treat sulfate-rich expansive soils for supporting pavement infrastructure. Low-sulfate and high-sulfate soils were prepared and treated with lime and different dosages of GP to study, understand, and compare their effects on the strength, durability, swelling–shrinkage strains, resilient moduli over different curing periods. Furthermore, microstructural studies using FESEM and XRD were performed to detect the formation of new reaction products and how they affect the properties of treated soils. Some of the salient findings from this study are presented below:

- The 30% GP treatment significantly improved unsoaked and soaked UCSs of LS and HS soils cured for different periods, compared with 6% lime treatment and 8% GP treatment. The uniformly-formed GP networks enhanced the bonds between GP gels and clay particles.
- The strength retention factors of 30% GP treatment were significantly higher than 6% lime treatment and 8% GP treatment for both soil groups. The higher strength retention factors after moisture intrusion for 30% GP treatment of HS soils compared with 6% lime treatment indicated the potential benefits of this eco-friendly stabilizer. The absence of ettringite crystals and strong GP networks from geopolymerization possibly contributed to the strength retention.

- The 30% GP treatment on LS and HS soils was effective in swell-shrinkage potential during all curing periods. However, for HS soils, the higher dosage of GP was more effective than 6% lime and lower GP dosage. For the shrinkage reduction, 30% GP treatment was more effective than 6% lime and 8% GP treatments.
- M_R values from RLTT indicated that 30% GP significantly improved the stiffness of the treated HS soils for various curing periods. Furthermore, GP dosage developed soil hardening behavior and improved shear resistance as compared with traditional lime treatment, indicating its efficacy for use as a subgrade stabilizer.
- Microstructural characterization using FESEM images detected the presence of needle-shaped ettringite crystals in the lime-treated HS soil. The presence of ettringite was also confirmed using characteristic peaks identified from XRD studies. The GP-treated soil showed uniform coatings of the GP network in the FESEM image. XRD diffractogram of the soil showed the absence of ettringite peaks indicating the potential efficacy of GP to suppress the ettringite formation and subsequently enhance engineering properties of high-sulfate expansive soils.

Future studies, including pavement test sections on GP-treated expansive soils, are required to close the knowledge gap between laboratory data and field implementations. Also, further studies on the strengthening mechanisms of the GP-clay system are needed to assess the long-term performance of GP-stabilized subgrade soils in ambient conditions. These would lead to a novel and sustainable binder for sulfate soil treatments.

Acknowledgments

The authors would like to thank the Transportation Consortium of South-Central States (Tran-SET)-Region 6's University Transportation Center (Award #19GTUTA01). The authors would also like to acknowledge the NSF I/UCRC program funded Center for Integration of Composites into Infrastructure (CICI) site at Texas A&M University, College Station, Award #2017796, Program Director: Dr. Prakash Balan. The authors would like to thank Dr. Sayantan Chakraborty and Krishneswar Ramineni for providing valuable inputs on this research at Texas A&M University.

Author Contributions

The authors confirm contribution to the paper as follows: study conception and design: J. Jang, N. Biswas, A. J. Puppala, S. S. C. Congress, M. Radovic; data collection: J. Jang, O. Huang; analysis and interpretation of results: J. Jang, N. Biswas, A. J. Puppala, S. S. C. Congress, M. Radovic, O. Huang; draft manuscript preparation: J. Jang, N. Biswas, A. J. Puppala, M. Radovic. All authors reviewed the results and approved the final version of the manuscript.

Declaration of Conflicting Interests

The author(s) declared no potential conflicts of interest with respect to the research, authorship, and/or publication of this article.

Funding

The author(s) disclosed receipt of the following financial support for the research, authorship, and/or publication of this article: the Transportation Consortium of South-Central States (Tran-SET)-Region 6's University Transportation Center (Award #19GTUTA01). NSF I/UCRC program funded Center for Integration of Composites into Infrastructure (CICI) site at Texas A&M University, College Station, Award #2017796.

ORCID iDs

Jungyeon Jang https://orcid.org/0000-0002-3739-6657
Nripojyoti Biswas https://orcid.org/0000-0001-5548-1292
Anand J. Puppala https://orcid.org/0000-0003-0435-6285
Surya Sarat Chandra Congress https://orcid.org/0000-0001-5921-9582
Oscar Huang https://orcid.org/0000-0001-7004-3506

References

1. Biswas, N., A. J. Puppala, M. A. Khan, S. S. C. Congress, A. Banerjee, and S. Chakraborty. Evaluating the Performance of Wicking Geotextile in Providing Drainage for Flexible Pavements Built Over Expansive Soils. *Transportation Research Record: Journal of the Transportation Research Board*, 2021. 2675: 208–221. https://doi.org/10.1177/03611981211001381.
2. Boluk, B., A. J. Puppala, S. Chakraborty, and P. Bhaskar. Forensic Analyses and Rehabilitation of a Failed Highway Embankment Slope in Texas. *Transportation Research Record: Journal of the Transportation Research Board*, 2021. 2675: 121–134. https://doi.org/10.1177/0361198121996359.
3. Hoyos, L. R., A. Laikram, and A. Puppala. Behavior of Chemically Stabilized Sulfate-Rich Expansive Clay Under Quick-Aging Environment. In *Proc., Ground Modification and Seismic Mitigation: GeoShanghai International Conference 2006* (Porbaha, A., S.-L. Shen, J. Wartman, and J.-C. Chai eds.), Shanghai, China, June 6–8, 2006, ASCE, Reston, VA, pp. 89–96. https://doi.org/10.1061/40864(196)13.
4. Biswas, N., S. Chakraborty, A. J. Puppala, and A. Banerjee. A Novel Method to Improve the Durability of Lime-Treated Expansive Soil. In The Indian Geotechnical Conference 2019 (Patel, S., C. H. Solanki, K. R. Reddy, and S. K. Shukla eds.), Springer, Singapore, 2021, pp. 227–238. https://doi.org/10.1007/978-981-33-6444-8_20.
5. Puppala, A. J. Performance Evaluation of Infrastructure on Problematic Expansive Soils: Characterization Challenges, Innovative Stabilization Designs, and Monitoring

Methods. *Journal of Geotechnical and Geoenvironmental Engineering*, Vol. 147, No. 8, 2021, pp. 1–15. https://doi.org/10.1061/(ASCE)GT.1943-5606.0002518.

6. Khan, A., N. Biswas, A. Banerjee, and A. J. Puppala. Performance of Geocell-Reinforced Recycled Asphalt Pavement (RAP) Bases in Flexible Pavements Built on Expansive Soils. In *Proc., Geotechnical Earthquake Engineering and Special Topics: Geo-Congress 2020* (Hambleton, J. P., R. Makhnenko, and A. S. Budge eds.), Minneapolis, MN, February 25–28, 2020, American Society of Civil Engineers, Reston, VA, pp. 488–497. https://doi.org/10.1061/9780784482810.051.
7. Little, D. N., S. Nair, and B. Herbert. Addressing Sulfate-Induced Heave in Lime Treated Soils. *Journal of Geotechnical and Geoenvironmental Engineering*, Vol. 136, No. 1, 2010, pp. 110–118. https://doi.org/10.1061/(ASCE)GT.1943-5606.0000185.
8. Little, D. N., and S. Nair. *NCHRP 145: Recommended Practice for Stabilization of Sulfate-Rich Subgrade Soils*. Transportation Research Board, Washington, D.C., 2009.
9. Puppala, A. J., J. A. Griffin, L. R. Hoyos, and S. Chomtid. Studies on Sulfate-Resistant Cement Stabilization Methods to Address Sulfate-Induced Soil Heave. *Journal of Geotechnical and Geoenvironmental Engineering*, Vol. 130, No. 4, 2004, pp. 391–402. https://doi.org/10.1061/(ASCE)1090-0241(2004)130:4(391).
10. Little, D. N., and S. Nair. *NCHRP 144: Recommended Practice for Stabilization of Subgrade Soils and Base Materials*. Transportation Research Board, Washington, D.C., 2009.
11. Chakraborty, S., and S. Nair. Impact of Different Hydrated Cementitious Phases on Moisture-Induced Damage in Lime-Stabilised Subgrade Soils. *Road Materials and Pavement Design*, Vol. 19, No. 6, 2018, pp. 1389–1405. https://doi.org/10.1080/14680629.2017.1314222.
12. Akula, P., S. R. Naik, and D. N. Little. Evaluating the Durability of Lime-Stabilized Soil Mixtures Using Soil Mineralogy and Computational Geochemistry. *Transportation Research Record: Journal of the Transportation Research Board*, 2021. 2675(9): 1469–1481. https://doi.org/10.1177/03611981211007848.
13. Little, D. N., B. Herbert, and S. N. Kunagalli. Ettringite Formation in Lime-Treated Soils. Establishing Thermodynamic Foundations for Engineering Practice. *Transportation Research Record: Journal of the Transportation Research Board*, 2005. 1936: 51–59. https://doi.org/10.1177/0361198105193600107.
14. Puppala, A. J., N. Intharasombat, and R. K. Vempati. Experimental Studies on Ettringite-Induced Heaving in Soils. *Journal of Geotechnical and Geoenvironmental Engineering*, Vol. 131, No. 3, 2005, pp. 325–337. https://doi.org/10.1061/(ASCE)1090-0241(2005)130:3(325).
15. Puppala, A. J., A. Pedarla, and A. Gaily. *Implementation: Mitigation of High Sulfate Soils in Texas: Development of Design and Construction Guidelines*. Texas Department of Transportation, Austin, 2016.
16. Nair, S., and D. Little. Water as the Key to Expansion of Ettringite in Cementitious Materials. *Transportation Research Record: Journal of the Transportation Research Board*, 2009. 2104: 55–62. https://doi.org/10.3141/2104-06.
17. Chakraborty, S., A. J. Puppala, and N. Biswas. Role of Crystalline Silica Admixture in Mitigating Ettringite-Induced Heave in Lime-Treated Sulfate-Rich Soils. *Géotechnique*, 2021, pp. 1–17. https://doi.org/10.1680/jgeot.20.P.154.
18. Puppala, A. J., and A. Cerato. Heave Distress Problems in Chemically-Treated Sulfate-Laden Materials. *Geo-Strata*, Vol. 10, No. 2, 2009, pp. 28–30.
19. Zhang, M., M. Zhao, G. Zhang, P. Nowak, A. Coen, and M. Tao. Calcium-Free Geopolymer as a Stabilizer for Sulfate-Rich Soils. *Applied Clay Science*, Vol. 108, 2015, pp. 199–207. https://doi.org/10.1016/j.clay.2015.02.029.
20. Consoli, N. C., E. J. Bittar Marin, R. A. Quiñónez, H. C. Scheuermann Filho, T. Miranda, and N. Cristelo. Effect of Mellowing and Coal Fly Ash Addition on Behavior of Sulfate-Rich Dispersive Clay After Lime Stabilization. *Journal of Materials in Civil Engineering*, Vol. 31, No. 6, 2019, p. 04019071. https://doi.org/10.1061/(ASCE)MT.1943-5533.0002699.
21. Harris, P., J. Von Holdt, S. Sebesta, and T. Scullion. Recommendations for Stabilization of High-Sulfate Soils in Texas. *Transportation Research Record: Journal of the Transportation Research Board*, 2006. 1952: 71–79. https://doi.org/10.1177/0361198106195200108.
22. Harris, J. P., S. Sebesta, and T. Scullion. Hydrated Lime Stabilization of Sulfate-Bearing Vertisols in Texas. *Transportation Research Record: Journal of the Transportation Research Board*, 2004. 1868: 31–39. https://doi.org/10.3141/1868-04.
23. Talluri, N., A. Puppala, B. Chittoori, A. Gaily, and P. Harris. Stabilization of High-Sulfate Soils by Extended Mellowing. *Transportation Research Record: Journal of the Transportation Research Board*, 2013. 2363: 96–104. https://doi.org/10.3141/2363-11.
24. Khadka, S. D., P. W. Jayawickrama, S. Senadheera, and B. Segvic. Stabilization of Highly Expansive Soils Containing Sulfate Using Metakaolin and Fly Ash Based Geopolymer Modified With Lime and Gypsum. *Transportation Geotechnics*, Vol. 23, 2020, p. 100327. https://doi.org/10.1016/j.trgeo.2020.100327.
25. Samuel, R., A. J. Puppala, A. Banerjee, O. Huang, M. Radovic, and S. Chakraborty. Improvement of Strength and Volume-Change Properties of Expansive Clays With Geopolymer Treatment. *Transportation Research Record: Journal of the Transportation Research Board*, 2021. 2675: 308–320. https://doi.org/10.1177/03611981211001842.
26. Samuel, R., A. J. Puppala, and M. Radovic. Sustainability Benefits Assessment of Metakaolin-Based Geopolymer Treatment of High Plasticity Clay. *Sustainability*, Vol. 12, No. 24, 2020, p. 10495. https://doi.org/10.3390/su122410495.
27. Santoni, R. L., J. S. Tingle, and S. L. Webster. Stabilization of Silty Sand With Nontraditional Additives. *Transportation Research Record: Journal of the Transportation Research Board*, 2002. 1787: 61–70. https://doi.org/10.3141/1787-07.

28. Jang, J., A. J. Puppala, S. Chakraborty, N. Biswas, O. Huang, and M. Radovic. Eco-Friendly Stabilization of Sulfate-Rich Expansive Soils Using Geopolymers for Transportation Infrastructure. In *Proc., Tran-SET 2021* (Hossain, Z., M. Hassan, and L. Mohammad, eds.), Virtually, June 3–4, 2021, American Society of Civil Engineers, Reston, VA, pp. 223–231. http://doi.org/10.1061/9780784483787.023.
29. Lizcano, M., A. Gonzalez, S. Basu, K. Lozano, and M. Radovic. Effects of Water Content and Chemical Composition on Structural Properties of Alkaline Activated Metakaolin-Based Geopolymers. *Journal of the American Ceramic Society*, Vol. 95, No. 7, 2012, pp. 2169–2177. https://doi.org/10.1111/j.1551-2916.2012.05184.x.
30. Yu, X., A. J. Puppala, M. Radovic, S. Chakraborty, J. Jang, and O. Huang. *Eco-Friendly Stabilization of Sulfate-Rich Expansive Soils Using Geopolymers for Transportation Infrastructure*. Transportation Consortium of South-Central States, 2020, pp. 1–35. https://rosap.ntl.bts.gov/view/dot/56560. Accessed December 1, 2020.
31. He, J., Y. Jie, J. Zhang, Y. Yu, and G. Zhang. Synthesis and Characterization of Red Mud and Rice Husk Ash-Based Geopolymer Composites. *Cement and Concrete Composites*, Vol. 37, No. 1, 2013, pp. 108–118. http://dx.doi.org/10.1016/j.cemconcomp.2012.11.010.
32. Temuujin, J., A. van Riessen, and R. Williams. Influence of Calcium Compounds on the Mechanical Properties of Fly Ash Geopolymer Pastes. *Journal of Hazardous Materials*, Vol. 167, No. 1–3, 2009, pp. 82–88. https://doi.org/10.1016/j.jhazmat.2008.12.121.
33. Khedmati, M., H. Alanazi, Y. R. Kim, G. Nsengiyumva, and S. Moussavi. Effects of Na2O/SiO2 Molar Ratio on Properties of Aggregate-Paste Interphase in Fly Ash-Based Geopolymer Mixtures Through Multiscale Measurements. *Construction and Building Materials*, Vol. 191, 2018, pp. 564–574. https://doi.org/10.1016/j.conbuildmat.2018.10.024.
34. Chowdary, B., V. Ramanamurty, and R. J. Pillai. Fiber Reinforced Geopolymer Treated Soft Clay – An Innovative and Sustainable Alternative for Soil Stabilization. *Materials Today: Proceedings*, Vol. 32, 2020, pp. 777–781. https://doi.org/10.1016/j.matpr.2020.03.574.
35. Yu, J., Y. Chen, G. Chen, and L. Wang. Experimental Study of the Feasibility of Using Anhydrous Sodium Metasilicate as a Geopolymer Activator for Soil Stabilization. *Engineering Geology*, Vol. 264, 2020, p. 105316. https://doi.org/10.1016/j.enggeo.2019.105316.
36. Rivera, J. F., A. Orobio, N. Cristelo, and R. M. de Gutiérrez. Fly Ash-Based Geopolymer as A4 Type Soil Stabiliser. *Transportation Geotechnics*, Vol. 25, 2020, p. 100409. https://doi.org/10.1016/j.trgeo.2020.100409.
37. Yaghoubi, M., A. Arulrajah, M. M. Disfani, S. Horpibulsuk, S. Darmawan, and J. Wang. Impact of Field Conditions on the Strength Development of a Geopolymer Stabilized Marine Clay. *Applied Clay Science*, Vol. 167, 2019, pp. 33–42. https://doi.org/10.1016/j.clay.2018.10.005.
38. Rios, S., N. Cristelo, A. Viana da Fonseca, and C. Ferreira. Structural Performance of Alkali-Activated Soil Ash versus Soil Cement. *Journal of Materials in Civil Engineering*, Vol. 28, No. 2, 2016, p. 04015125. https://doi.org/10.1061/(ASCE)MT.1943-5533.0001398.
39. Phetchuay, C., S. Horpibulsuk, C. Suksiripattanapong, A. Chinkulkijniwat, A. Arulrajah, and M. M. Disfani. Calcium Carbide Residue: Alkaline Activator for Clay-Fly Ash Geopolymer. *Construction and Building Materials*, Vol. 69, 2014, pp. 285–294. http://dx.doi.org/10.1016/j.conbuildmat.2014.07.018.
40. Cristelo, N., S. Glendinning, L. Fernandes, and A. T. Pinto. Effect of Calcium Content on Soil Stabilisation With Alkaline Activation. *Construction and Building Materials*, Vol. 29, 2012, pp. 167–174. http://dx.doi.org/10.1016/j.conbuildmat.2011.10.049.
41. TxDOT. *Treatment Guidelines for Soils and Base in Pavement Structures*. Texas Department of Transportation. https://ftp.dot.state.tx.us/pub/txdot/mtd/treatment-guidelines.pdf. Accessed April 5, 2022.
42. Lizcano, M., H. S. Kim, S. Basu, and M. Radovic. Mechanical Properties of Sodium and Potassium Activated Metakaolin-Based Geopolymers. *Journal of Materials Science*, Vol. 47, No. 6, 2012, pp. 2607–2616. https://doi.org/10.1007/s10853-011-6085-4.
43. Amran, Y. H. M., R. Alyousef, H. Alabduljabbar, and M. El-Zeadani. Clean Production and Properties of Geopolymer Concrete; A Review. *Journal of Cleaner Production*, Vol. 251, 2020, p. 119679. https://doi.org/10.1016/j.jclepro.2019.119679.
44. Bing-hui, M., H. Zhu, C. Xue-min, H. Yan, and G. Si-yu. Effect of Curing Temperature on Geopolymerization of Metakaolin-Based Geopolymers. *Applied Clay Science*, Vol. 99, 2014, pp. 144–148. http://dx.doi.org/10.1016/j.clay.2014.06.024.
45. Biswas, N., A. J. Puppala, S. Chakraborty, and M. A. Khan. Utilization of Silica-Based Admixture to Improve the Durability of Lime-Treated Expansive Soil. In *Proc., Earth Retention, Ground Improvement, and Seepage Control: IFCEE 2021* (El Mohtar, C., S. Kulesza, T. Baser, and M. D. Venezia eds.), Dallas, TX, May 10–14, 2021, ASCE, Reston, VA, pp. 233–242. https://ascelibrary.org/doi/abs/10.1061/9780784483411.023.
46. NCHRP. *Guide for Mechanistic-Empirical Design of New and Rehabilitated Pavement Structures*. Project 1-37A. National Cooperative Highway Research Program, Washington, D.C., 2004.
47. Andrei, D., M. W. Witczak, C. W. Schwartz, and J. Uzan. Harmonized Resilient Modulus Test Method for Unbound Pavement Materials. *Transportation Research Record: Journal of the Transportation Research Board*, 2004. 1874: 29–37. https://doi.org/10.3141/1874-0.
48. Goldstein, J. I., D. E. Newbury, J. R. Michael, N. W. M. Ritchie, J. H. J. Scott, and D. C. Joy. *Scanning Electron Microscopy and X-Ray Microanalysis*. Springer, New York, NY, 2018, p. 550.